Dynamics of a vesicle in general flow – Supplementary Note: Numerical simulations of the microfluidic "four-roll equivalent" chamber

We simulated numerically the flow field within the microchannel used in our experiment. The purpose of the simulation was twofold: first, we needed to assess with a fully three dimensional simulation, the true amount of nonuniformity of the flow off the center of the test chamber, and its deviation from the planar linear flow assumed by the theory for the dynamical regimes of the vesicles. The simulations of this microfluidic configuration, done by Lee et al., *Applied Physics Letters* **90**, 074103 (2007), which inspired our work, were done with the somewhat questionable assumption that the flow is planar at any height and has a parabolic z-dependence. Vertical velocities are indeed present, and are important for determining the residence time of the vesicle in the focal observation plane. Secondly, we needed to assess the robustness of the flow configurations with respect to imperfections of fabrication of the microchannel, either because of defects in the etching of the SU8 positive mold, or because of deformations in the PDMS channel. We typically expected variances from the design shape of the order of several micrometers.

The simulations were carried out in Comsol v3.5 (COMSOL, Inc., www.comsol.com). In order to assess the effect of geometrical imperfections, we simulated a reference channel and a few variations of it. The reference channel for the simulations featured a central test chamber with radius 240μm and height $h = 320\mu$m. The edges of the stems dividing the test chamber from the inflow and outflow channels were filleted with a curvature radius of 10μm. The domain was meshed by first triangulating the planform of the test chamber in the xy plane. The 3d mesh is obtained by extruding the plane mesh on 10 layers (see figure 1).

Constant pressure boundary conditions are imposed to the eight channel cross-sections, and no-slip conditions on any other wall. Notably, numbering the inlets and outlets of the channel in counterclockwise order, the pressures given were:

$$\begin{aligned} p_2 = p_4 = p_6 = p_8 &= P_1 \\ p_3 = p_7 &= P_1 + P_0 \\ p_1 = p_5 &= P_1 + \Delta P \end{aligned}$$

where $P_0 = 1$Pa (much smaller than the reference P measured outside of the experimental channel, which accounts for all the head losses in the hydraulic paths) and $\Delta P = (1-a)P_0$, with $a = 0 \div 1$. In the simulation the fluid was assigned a density of $\rho = 1000\text{kg/m}^3$ and a viscosity $\eta = 1\text{mPa/s}$. At such low Reynolds number, anyway, all flow

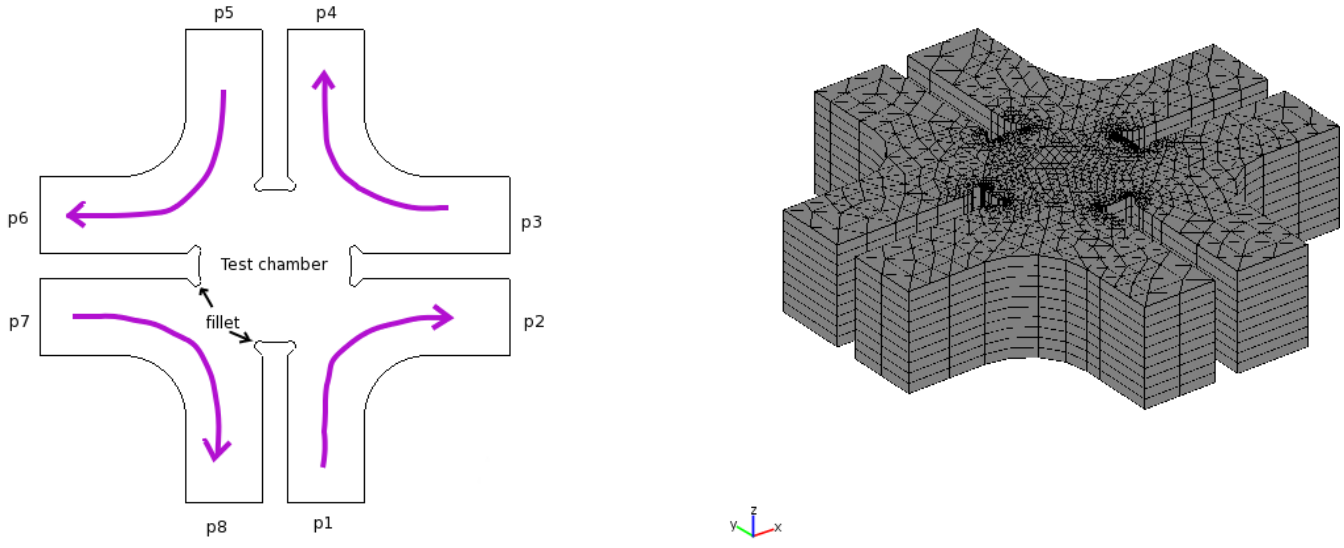

(a) planar scheme of the channel

(b) 3d view of the computational mesh

Figure 1: the simulation domain

velocities are supposed to be linearly proportional to the pressures and inversely proportional to η. Different flow configurations are realized changing the pressure inbalance parameter a. In the midplane, a general (linear, planar) flow is characterised by the parameter

$$f = \frac{s - \omega}{s + \omega}$$

($f = -1 \div 1$), where $s = \sqrt{u_x^2 + v_y^2 + \frac{1}{2}(u_y + v_x)^2}$ is the strain rate and $\omega = \frac{1}{2}|u_y - v_x|$ is the vertical component of the vorticity.

A flow with $f = -1$ is purely rotational, with $f = 0$ is a shear and with $f = 1$ is elongational. Almost purely rotational flow in the center of the test chamber is achieved for $a = 1$.

Plots of the resulting flow field, with highlighted streamlines and values of the function f on selected slices of the volume, are presented in the following, for the reference geometry.

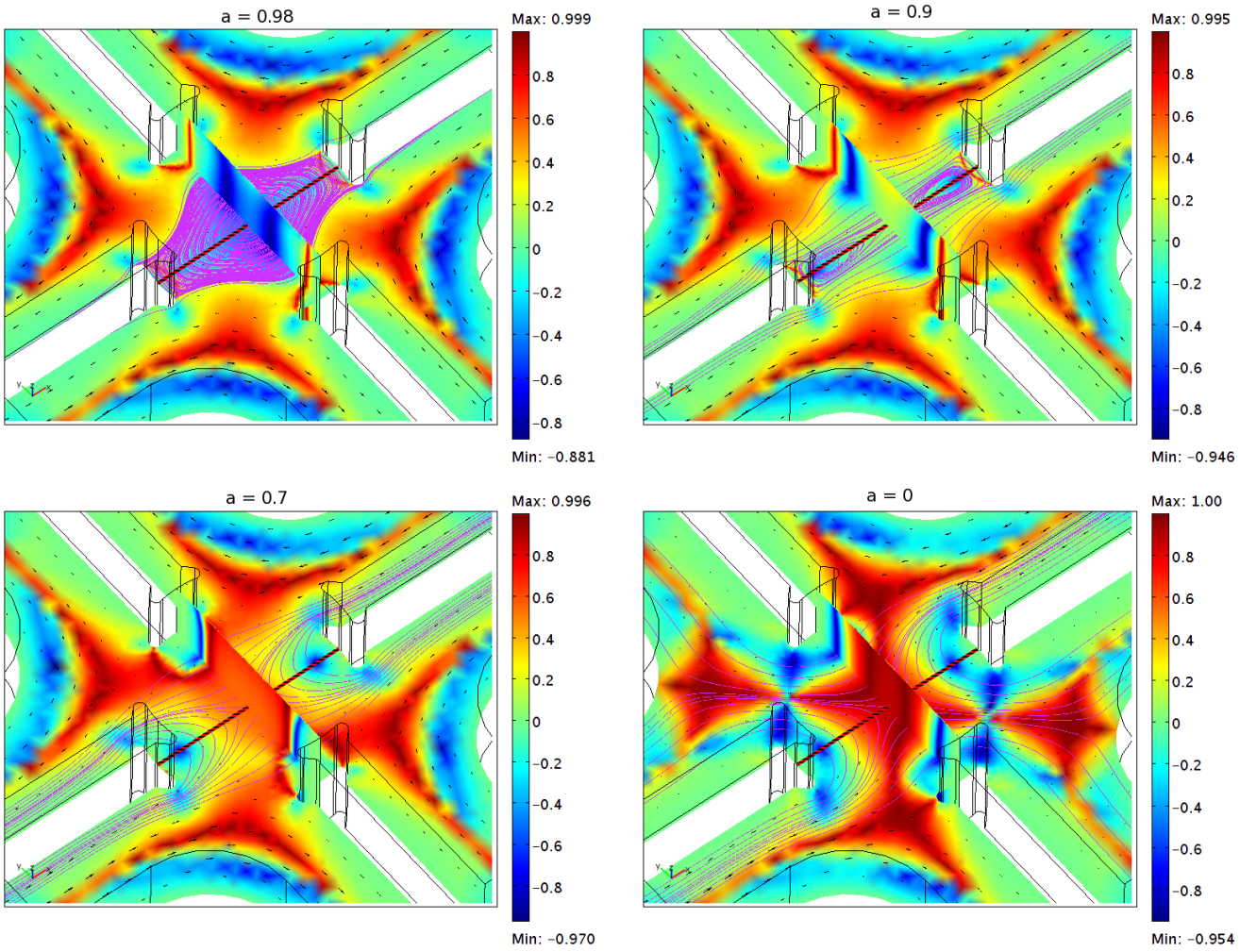

Figure 2: Flow field inside the test chamber for various values of a. The colormap depicts the values of f on the mid-height plane and on a vertical section of the device, and some streamlines on the midplane are shown to illustrate the topology of the flow.

The flow properties depend on position within the test chamber. To illustrate the typical variations, we plot in figures 3,4 typical cross sections of f and w in the mid plane, as well as along the depth. The three-dimensional effect of vertical secondary motions is evidenced in figure 5, where selected streamlines originating from points along the dashed red/black line in the figures 2 are followed for long times.

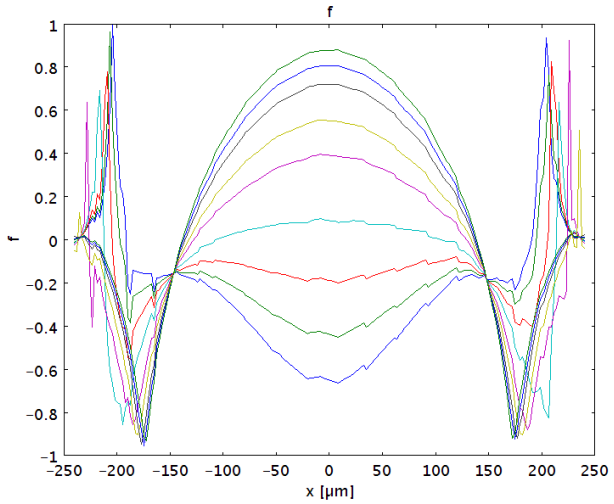

(a) cross section along the dashed red/black line in the figures 2

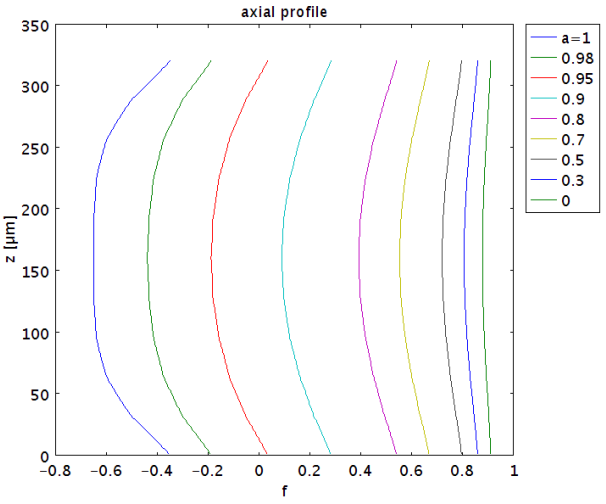

(b) along the vertical axis of the test chamber

Figure 3: Spatial variation of f inside the test chamber for various values of a

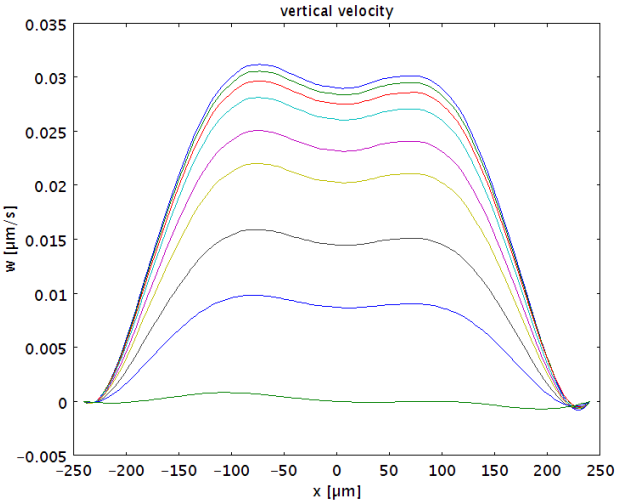

(a) cross section along the dashed red/black line in the figures 2

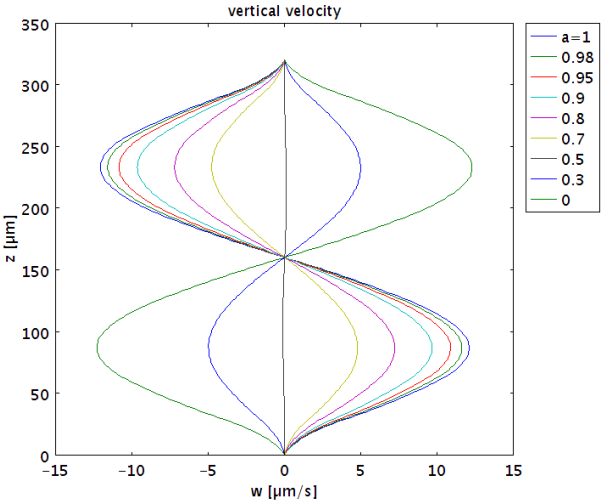

(b) along the vertical axis of the test chamber

Figure 4: Spatial variation of the vertical component of the velocity w inside the test chamber for various values of a. Note that the values imply that while the flow is essentially planar in the mid plane, the equilibrium in the center may be stable or unstable depending on the value of a.

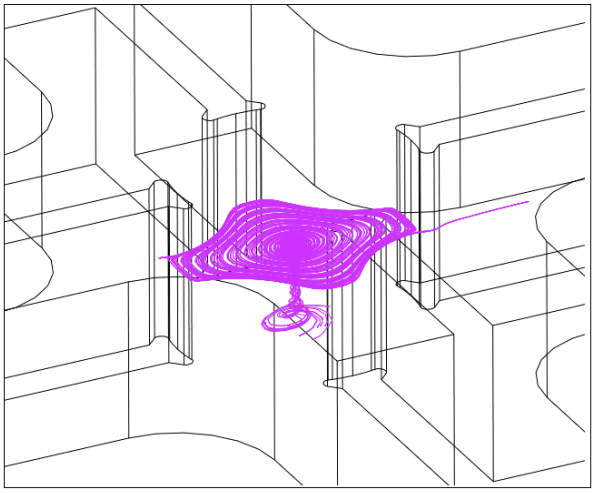

Figure 5: Secondary long term motion due to non vanishing vertical velocity in the bulk of the test chamber, for $a = 1$, evidenced by drawing streamlines originating from selected points in the mid-plane.

The sensitivity of the setup to fabrication imperfections has been also tested, by simulating various similar symmetrical and non symmetrical (imperfect) configurations, with different test chamber diameters, different stem fillet radii. Channels of 200 to 400µm height have been examined. Here we compare five symmetric cases, and a non symmetrical one: figure 6a shows data for A)–C) $h = 320\mu$m, edge fillets respectively of $r = 10\mu$m, $r = 7\mu$m and $r = 3\mu$m; D) $h = 300\mu$m, edge fillets of $r = 7\mu$m; E) $h = 200\mu$m, edge fillets of $r = 3\mu$m; F) $h = 320\mu$m, seven out of eight edge fillets with $r = 10\mu$m and one with $r = 3\mu$m. It is clear that geometrical variations translate into different profiles of $f(1 - \Delta P/P_0)$ roughly of the same magnitude of the discrepancy observed between calculated and simulated data, thought no specifical attempt to match the experimental profile was made, due to the too many possible geometrical dimensions to perturb.

In figure 6b the values of $a = 1$ and $a = 0.9$ are picked for comparison because the former corresponds for all cases to the most rotational flow configuration, whereas the value of $a = 0.9$ gives in the first two cases approximately a shear flow, in which the velocity at the center should not depend on x.

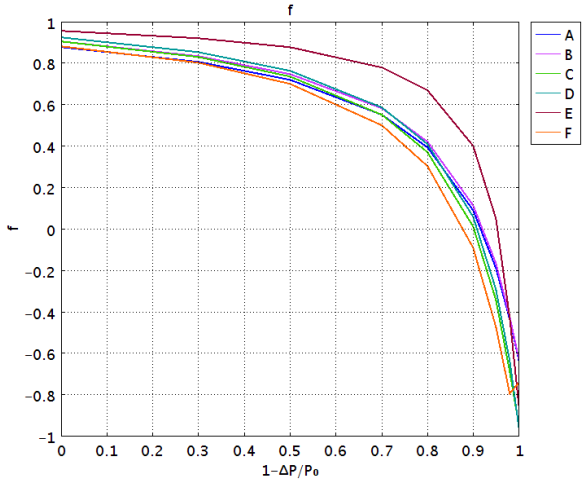

(a) Value of f in the center of the test chamber, mid height, as function of a; geometries A) – F) described in the text.

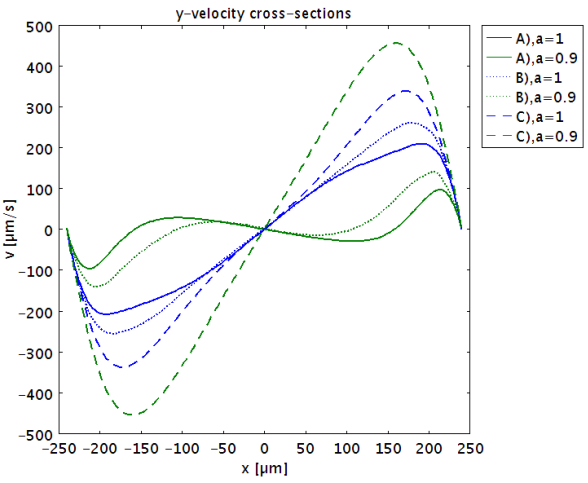

(b) Value of the y component of the velocity in the mid-plane, cross section along the dashed red/black line in the figures 2, for a=1 (blue) and $a = 0.9$ (green), for cases A)–C).

Figure 6: Comparison of three channel geometries